Massive quark propagator and competition between chiral and diquark condensate

Mei Huang* and Pengfei Zhuang†
Physics Department, Tsinghua University, Beijing 100084, China

Weiqin Chao‡
CCAST, Beijing 100080, China and Institute of High Energy Physics, Chinese Academy of Sciences, Beijing 100039, China

(Received 16 October 2001; revised manuscript received 10 December 2001; published 5 April 2002)

The Green-function approach is extended to the moderate baryon density region in the framework of an extended Nambu–Jona-Lasinio model, and the thermodynamic potential with both chiral and diquark condensates evaluated by using the massive quark propagator. The phase structure along the chemical potential direction is investigated and the strong competition between the chiral and diquark condensate is analyzed by investigating the influence of the diquark condensate on the sharp Fermi surface. The influence of the diquark condensate on the quark properties is investigated, even though the quarks in the color-breaking phase are very different from those in the chiral-breaking phase; the difference between quarks in different colors is very small.

DOI: 10.1103/PhysRevD.65.076012 PACS number(s): 11.15.Ex, 12.38.Aw, 26.60.+c

I. INTRODUCTION

QCD phase transitions along the baryon density direction attracted much attention recently since it was found that the color-superconducting gap can be of the order of 100 MeV [1,2], which is two orders larger than early perturbative estimations [3]. However, up until now, there has been no uniform framework discussing the phase structure in the wide region of chemical potential μ from about 300 to 10^8 MeV.

In the idealized case at asymptotically high baryon densities, the color superconductivity with two massless flavors and the color-flavor-locking (CFL) phase with three degenerate massless quarks have been widely discussed from first principles QCD calculations, see [4] and references therein. Usually, the diagrammatic methods are used in the asymptotic densities. The Green function of the eight-component field and the gap equation were discussed in detail in [5–7]. Neither the current quark mass nor the chiral condensate are necessary to be considered because they can be neglected compared with the very high Fermi surface. At less-than-asymptotic densities, the corrections of nonzero quark mass to the pure CFL phase can be treated perturbatively by expanding the current quark mass around the chiral limit [8,9].

For physical applications we are more interested in the moderate baryon density region, which may be related to the neutron stars and, in very optimistic cases, even to heavy-ion collisions. Usually, effective models such as the instanton, as well as the Nambu–Jona-Lasinio (NJL) model, are used. The model parameters are fixed in the QCD vacuum. In this region, the usual way is to use the variational methods working out the gap equations from the thermodynamic potential [10–23], except for [13] and [16] in the instanton model, where the quark propagator was evaluated explicitly but the form is complicated.

One of our main aims in this paper is to apply the Green-function approach in the moderate baryon density region. To work out the phase structure from hadron phase to the color superconducting phase, one should deal with the chiral condensate and diquark condensate simultaneously. Because the chiral condensation contributes a dynamic quark mass, it is not reasonable any more in this density region to treat the quark mass term perturbatively, like in [9]. By using the energy projectors for massive quark, we will evaluate the Nambu-Gorkov massive quark propagator, which will help us deal with the chiral and diquark condensate simultaneously.

In the normal phase, the quarks in different colors are degenerate, while in the color-breaking phase, it is natural to assume that the quarks involved in the diquark condensate are different from that not participating in the diquark condensate. In [13] and [16], different masses for the quarks which participate and not participate in the diquark condensate are introduced. However, we will see that it is difficult to get the mass expression for the quarks participating in the diquark condensate, because the particles and holes mix with each other and the elementary excitations are quasiparticles and quasiholes near the Fermi surface. In our case, the difference between quarks in different colors has been reflected by their propagators; we read the difference through calculating the quarks' chiral condensate, but did not try to work out their masses. In the chiral limit, the chiral condensate disappears entirely in the color superconducting phase; it is not possible to investigate the influence of color breaking on quarks in different colors, so we will keep the current quark mass finite in this paper.

In the moderate baryon density region people are interested in the question whether there exists a region where both the chiral symmetry and color symmetry are broken [10–15]. In the chiral limit it was found that the existence of the mixed broken phase depends on the coupling constants G_S and G_D in the quark antiquark and diquark channels

*Electronic address: huangmei@mail.tsinghua.edu.cn
†Electronic address: zhuangpf@mail.tsinghua.edu.cn
‡Electronic address: chaowq@hp.ccast.ac.cn

[12,14]. In the case of a small ratio of $G_D/G_S<1$ the calculations in the instanton model [10,11], the NJL model [12], and the random matrix model [14] show a strong competition between the chiral and diquark condensates, i.e., where one condensate is nonzero the other vanishes. While for $G_D/G_S>1$ the calculations in the random matrix model [14] and the NJL model [12] show that there exists a region where both chiral (dynamical) symmetry and color symmetry are broken, and the chiral and diquark condensate coexist. The larger the value of G_D/G_S is, the wider the region of the mixed broken phase that has been found in the random matrix model [14].

The presence of a small current quark mass will induce chiral symmetry that only restores partially and there will always exist a small chiral condensate in the color superconducting phase, this phenomena had been called the coexistence of chiral and diquark condensates in [10,11]. In order to differ from this coexistence of the diquark and the small chiral condensate induced by current quark mass, we will call the coexistence region of the diquark and large chiral condensate induced by large G_D/G_S before the chiral phase transition the mixed broken phase.

In the coexistence region resulting from the current quark mass, the chiral condensate is small compared with the diquark condensate, and the role of the chiral condensate can be prescribed by the Anderson theroem [15], i.e., in this phase, the contribution of the chiral condensate to thermodynamic quantities becomes strongly suppressed, and one can calculate the diquark condensate and neglect the influence of the chiral condensate.

In this paper we will explain the existence of the mixed broken phase induced by larger G_D/G_s by analyzing the influence of the diquark condensate on the Fermi surface. In the mean-field approximation of the NJL model, the thermal system of the constituent quarks is a nearly ideal Fermi gas, and there is a sharp Fermi surface. The chiral symmetry begins to restore when the chemical potential is larger than the quark mass in the vacuum. When a diquark condensate is formed, the Cooper pair extends the Fermi surface, which induces the chiral symmetry to restore at a smaller chemical potential. The stronger the coupling constant in the diquark channel, the larger the diquark condensate and the smoother the Fermi surface.

In the following, we briefly introduce the extended NJL model in Sec. II, then in Sec III we evaluate the thermodynamic potential using the massive quark propagator. In Sec. IV we get the gap equations and condensates. The numerical results and conclusions are given in Sec. V.

II. THE EXTENDED NJL MODEL

The choice of the NJL model [24] is motivated by the fact that this model displays the same symmetries as QCD and that it describes well the spontaneous breakdown of chiral symmetry in the vacuum and its restoration at high temperature and density. The model we used in this paper is an extended version of the two-flavor NJL model, including interactions in the color singlet quark-antiquark channel and the color antitriplet diquark channel, which is not directly extended from the NJL model, but from the QCD Lagrangian [25–27].

The importance of color $\bar{3}$ diquark degree of freedom is related to the fact that one can construct a color-singlet nucleon current based on it. Because the gluon exchange between two quarks in the color $\bar{3}$ channel is attractive, one can view a color-singlet baryon as a quark-diquark bound state. And experimental data from pp collisions indicate the existence of this quark-diquark component in nucleons.

The first attempt to investigate the diquark properties in the NJL model was taken in [28]. Starting from an NJL model for scalar, pseudoscalar, vector, and axial-vector interactions of the $(\bar{q}q)\times(\bar{q}q)$ type and Fierz-transforming away the vector and axial-vector interactions, the scalar and pseudoscalar mesons, and diquarks can be obtained. However, this method could not get a consistent treatment of vector and axial-vector particles.

The extended NJL model we used was derived directly from QCD Lagrangian [25,26]. Integrating out gluon degrees of freedom from the QCD Lagrangian, and performing a local approximation for the (nonperturbative) gluon propagator, one gets a contact current-current interaction. By using a special Fierz rearrangement [29], one can completely decompose the two-quark-current interaction term into ''attractive'' color-singlet $(\bar{q}q)$ and color-antitriplet (qq) channels. In this way, a complete simultaneous description of scalar, pseudoscalar, vector, and axial-vector mesons and diquarks is possible, thus the extended NJL model including $(\bar{q}q)\times(\bar{q}q)$ interactions is completed by a corresponding $(\bar{q}\bar{q})\times(qq)$ interaction part.

In our present work we only consider scalar, pseudoscalar mesons, and scalar diquarks, and we use the following Lagrangian density:

$$\mathcal{L}=\bar{q}(i\gamma^\mu\partial_\mu-m_0)q+G_S[(\bar{q}q)^2+(\bar{q}i\gamma_5\vec{\tau}q)^2] + G_D[(i\bar{q}^C\varepsilon\epsilon^b\gamma_5 q)(i\bar{q}\varepsilon\epsilon^b\gamma_5 q^C)], \quad (1)$$

where $q^C=C\bar{q}^T$, $\bar{q}^C=q^TC$ are charge-conjugate spinors, $C=i\gamma^2\gamma^0$ is the charge conjugation matrix (the superscript T denotes the transposition operation), m_0 is the current quark mass, the quark field $q\equiv q_{i\alpha}$ with $i=1,2$ and $\alpha=1,2,3$ is a flavor doublet and color triplet, as well as a four-component Dirac spinor, $\vec{\tau}=(\tau^1,\tau^2,\tau^3)$ are Pauli matrices in the flavor space, where τ^2 is antisymmetric, and $(\varepsilon)^{ik}\equiv\varepsilon^{ik}$, $(\epsilon^b)^{\alpha\beta}\equiv\epsilon^{\alpha\beta b}$ are totally antisymmetric tensors in the flavor and color spaces.

In Eq. (1), G_S and G_D are independent effective coupling constants in the scalar quark-antiquark and scalar diquark channels. The former is responsible for the meson excitations, and the latter for the diquark excitations, which in principle can be determined by fitting mesons' and baryons' properties in the vacuum. The attractive interaction in different channels in this Lagrangian will give rise to a very rich structure of the phase diagram. At zero temperature and density, the attractive interaction in the color singlet channel is responsible for the appearance of a quark antiquark condensate and for the spontaneous breakdown of the chiral sym-

metry, and the interaction in the qq channel binds quarks into diquarks (and baryons), but is not strong enough to induce diquark condensation. As the density increases, Pauli blocking suppresses the $\bar{q}q$ interaction, while the attractive interaction in the color antitriplet diquark channel will induce the quark-quark condensate around the Fermi surface which can be identified as a superconducting phase.

After bosonization [25,26], one can obtain the linearized version of the model (1):

$$\begin{aligned}\tilde{\mathcal{L}}=&\bar{q}(i\gamma^\mu\partial_\mu-m_0)q-\bar{q}(\sigma+i\gamma^5\vec{\tau}\vec{\pi})q\\&-\frac{1}{2}\Delta^{*b}(i\bar{q}^C\varepsilon\epsilon^b\gamma_5 q)-\frac{1}{2}\Delta^b(i\bar{q}\varepsilon\epsilon^b\gamma_5 q^C)\\&-\frac{\sigma^2+\vec{\pi}^2}{4G_S}-\frac{\Delta^{*b}\Delta^b}{4G_D},\end{aligned}\tag{2}$$

with the bosonic fields

$$\begin{aligned}&\Delta^b\sim i\bar{q}^C\varepsilon\epsilon^b\gamma_5 q,\quad \Delta^{*b}\sim i\bar{q}\varepsilon\epsilon^b\gamma_5 q^C,\\&\sigma\sim\bar{q}q,\quad \vec{\pi}\sim i\bar{q}\gamma^5\vec{\tau}q.\end{aligned}\tag{3}$$

Clearly, the σ and $\vec{\pi}$ fields are color singlets, and the diquark fields Δ^b and Δ^{*b} are color antitriplet and (isoscalar) singlets under the chiral $SU(2)_L\times SU(2)_R$ group. $\sigma\neq 0$ and $\Delta^b\neq 0$ indicate that chiral symmetry and color symmetry are spontaneously broken. We assume that the two condensates coexist i.e.,

$$\begin{aligned}&\sigma\neq 0,\quad \vec{\pi}=0,\\&\Delta^1=\Delta^2=0,\quad \Delta^3\neq 0.\end{aligned}\tag{4}$$

Here it has been regarded that only the first two colors participate in the condensate, while the third one does not. In the later expressions, we will simply use $\Delta\equiv\Delta^3$.

The real vacuum will be determined by the minimum of the thermodynamic potential at $T=0$ and $\mu=0$, and the minimum of the thermodynamic potential at any T,μ determines the stable state at that point.

III. PARTITION FUNCTION AND THERMODYNAMIC POTENTIAL

A. Nambu-Gorkov formalism

The partition function of the grand canonical ensemble can be evaluated by using the standard method [30,31]:

$$\mathcal{Z}=N'\int[d\bar{q}][dq]\exp\left\{\int_0^\beta d\tau\int d^3\vec{x}(\tilde{\mathcal{L}}+\mu\bar{q}\gamma_0 q)\right\},\tag{5}$$

where μ is the chemical potential, and $\beta=1/T$ is the inverse of temperature T.

According to the mean field approximation Eq. (4), we can write the partition function as a product of three parts,

$$\mathcal{Z}=\mathcal{Z}_{const}\mathcal{Z}_{q_{1,2}}\mathcal{Z}_{q_3}.\tag{6}$$

The constant part is

$$\mathcal{Z}_{const}=N'\exp\left\{-\int_0^\beta d\tau\int d^3\vec{x}\left[\frac{\sigma^2}{4G_S}+\frac{\Delta^*\Delta}{4G_D}\right]\right\}.\tag{7}$$

For the quarks in the first two colors (named as ''the first two quarks'' in the following) $Q=q_{1,2}$ participating in the quark condensate, one has

$$\begin{aligned}\mathcal{Z}_{q_{1,2}}=&\int[d\bar{Q}][dQ]\exp\left\{\int_0^\beta d\tau\int d^3\vec{x}\right.\\&\times\left[\frac{1}{2}\bar{Q}(i\gamma^\mu\partial_\mu-m+\mu)Q+\frac{1}{2}\bar{Q}^C(i\gamma^\mu\partial_\mu-m-\mu)Q^C\right.\\&\left.\left.+\frac{1}{2}\bar{Q}\Delta^-Q^C+\frac{1}{2}\bar{Q}^C\Delta^+Q\right]\right\}.\end{aligned}\tag{8}$$

Here we have introduced the constituent quark mass

$$m=m_0+\sigma,\tag{9}$$

and defined $\Delta^\pm$ as

$$\Delta^-=-i\Delta\varepsilon\epsilon^b\gamma_5,\quad \Delta^+=-i\Delta^*\varepsilon\epsilon^b\gamma_5\tag{10}$$

with the relation $\Delta^+=\gamma^0(\Delta^-)^\dagger\gamma^0$.

For the quark in the third color (named as ''the third quark'' in the following), which is not involved in the diquark condensate, one has

$$\begin{aligned}\mathcal{Z}_{q_3}=&\int[d\bar{q}_3][dq_3]\exp\left\{\int_0^\beta d\tau\int d^3\vec{x}\right.\\&\times\left[\frac{1}{2}\bar{q}_3(i\gamma^\mu\partial_\mu-m+\mu)q_3\right.\\&\left.\left.+\frac{1}{2}\bar{q}_3^C(i\gamma^\mu\partial_\mu-m-\mu)q_3^C\right]\right\}.\end{aligned}\tag{11}$$

Introducing the 8-component spinors for the third quark and the first two quarks, respectively,

$$\Psi_3=\begin{pmatrix}q_3\\q_3^C\end{pmatrix},\quad \bar{\Psi}_3=(\bar{q}_3\quad \bar{q}_3^C),\tag{12}$$

$$\Psi=\begin{pmatrix}Q\\Q^C\end{pmatrix},\quad \bar{\Psi}=(\bar{Q}\quad \bar{Q}^C),\tag{13}$$

and using the Fourier transformation in the momentum space,

$$q(x)=\frac{1}{\sqrt{V}}\sum_n\sum_{\vec{p}}e^{-i(\omega_n\tau-\vec{p}\cdot\vec{x})}q(\vec{p}),\tag{14}$$

where V is the volume of the thermal system, we can rewrite the partition function Eqs. (8) and (11) in the momentum space as

$$\mathcal{Z}_{q_{1,2}}=\int [d\Psi]\exp\left\{\frac{1}{2}\sum_{n,p}\bar{\Psi}\frac{\mathrm{G}^{-1}}{T}\Psi\right\}$$
$$=\mathrm{Det}^{1/2}(\beta\mathrm{G}^{-1}) \tag{15}$$

and

$$\mathcal{Z}_{q_3}=\int [d\Psi_3]\exp\left\{\frac{1}{2}\sum_{n,p}\bar{\Psi}_3\frac{G_0^{-1}}{T}\Psi_3\right\}$$
$$=\mathrm{Det}^{1/2}(\beta G_0^{-1}), \tag{16}$$

where the determinantal operation Det is to be carried out over the Dirac, color, flavor, and the momentum-frequency space. In Eqs. (15) and (16), we have defined the quark propagator in the normal phase

$$\mathrm{G}_0^{-1}=\begin{pmatrix}[G_0^+]^{-1} & 0\\ 0 & [G_0^-]^{-1}\end{pmatrix}, \tag{17}$$

with

$$[G_0^\pm]^{-1}=(p_0\pm\mu)\gamma_0-\vec{\gamma}\cdot\vec{p}-m \tag{18}$$

and $p_0=i\omega_n$, and the quark propagator in the color-breaking phase

$$\mathrm{G}^{-1}=\begin{pmatrix}[G_0^+]^{-1} & \Delta^-\\ \Delta^+ & [G_0^-]^{-1}\end{pmatrix}. \tag{19}$$

The Nambu-Gorkov propagator $\mathrm{G}(p)$ is determined from solving $1=\mathrm{G}^{-1}\,\mathrm{G}$, resulting in

$$\mathrm{G}=\begin{pmatrix}G^+ & \Xi^-\\ \Xi^+ & G^-\end{pmatrix}, \tag{20}$$

with the components

$$G^\pm\equiv\{[G_0^\pm]^{-1}-\Sigma^\pm\}^{-1},\quad \Sigma^\pm\equiv\Delta^\mp G_0^\mp\Delta^\pm,$$
$$\Xi^\pm\equiv-G^\mp\Delta^\pm G_0^\pm=-G_0^\mp\Delta^\pm G^\pm. \tag{21}$$

Here all components depend on the 4-momentum p^μ.

In the case of the mass term $m=0$, i.e., both the current quark mass m_0 and the chiral condensate $\langle\sigma\rangle$ are zero, the Nambu-Gorkov quark propogator has a simple form which could be derived from the energy projectors for massless particles [5,6], while if there is a small mass term, the quark propagator can be expanded perturbatively around $m=0$, but its form is very complicated [9]. In our case the quark mass term cannot be treated perturbatively; we have to find a general way to deal with the massive quark propagator.

Fortunately, we can evaluate a simple form for the massive quark propagator by using the energy projectors for massive particles. The energy projectors onto states of positive and negative energy for free massive particles are defined as

$$\Lambda_\pm(\vec{p})=\frac{1}{2}\left(1\pm\frac{\gamma_0(\vec{\gamma}\cdot\vec{p}+m)}{E_p}\right), \tag{22}$$

where the quark energy $E_p=\sqrt{\vec{p}^2+m^2}$. Under the transformation of γ_0 and γ_5, we can get another two energy projectors $\tilde{\Lambda}_\pm$,

$$\tilde{\Lambda}_\pm(\vec{p})=\frac{1}{2}\left(1\pm\frac{\gamma_0(\vec{\gamma}\cdot\vec{p}-m)}{E_p}\right), \tag{23}$$

which satisfy

$$\gamma_0\Lambda_\pm(\vec{p})\gamma_0=\tilde{\Lambda}_\mp(\vec{p}),\quad \gamma_5\Lambda_\pm(\vec{p})\gamma_5=\tilde{\Lambda}_\pm(\vec{p}). \tag{24}$$

The normal quark propagator elements can be rewritten as

$$G_0^\pm=\frac{\gamma_0\tilde{\Lambda}_+}{p_0+E_p^\pm}+\frac{\gamma_0\tilde{\Lambda}_-}{p_0-E_p^\mp}, \tag{25}$$

with $E_p^\pm=E_p\pm\mu$. The propagator has four poles, i.e.,

$$p_0=\pm E_p^-,\qquad p_0=\mp E_p^+, \tag{26}$$

where the former two correspond to the excitation energies of particles and holes, and the latter two are for antiparticles and antiholes, respectively.

The quark propagator, including the diquark condensate's contribution, can be evaluated as

$$G^\pm=\left(\frac{p_0-E_p^\pm}{p_0^2-E_\Delta^{\pm2}}\gamma_0\tilde{\Lambda}_++\frac{p_0+E_p^\mp}{p_0^2-E_\Delta^{\mp2}}\gamma_0\tilde{\Lambda}_-\right)$$
$$\times(\delta_{\alpha\beta}-\delta_{\alpha3}\delta_{\beta3})\delta^{ij} \tag{27}$$

and

$$\Xi^\pm=\left(\frac{\Delta^\pm}{p_0^2-E_\Delta^{\pm2}}\tilde{\Lambda}_+ +\frac{\Delta^\pm}{p_0^2-E_\Delta^{\mp2}}\tilde{\Lambda}_-\right), \tag{28}$$

with $E_\Delta^{\pm2}=E_p^{\pm2}+\Delta^2$. This propagator is very similar to the massless propagator derived in [5].

From the Nambu-Gorkov propagator, it is difficult to obtain the mass of the quark which participates in the diquark condensate. The four poles of the Nambu-Gorkov propagator, i.e.,

$$p_0=\pm E_\Delta^-,\qquad p_0=\mp E_\Delta^+, \tag{29}$$

correspond to the excitation energies of quasiparticles (quasiholes) and quasiantiparticles (quasiantiholes) in the color-breaking phase. These quasiparticles are superpositions of particles and holes.

We plot the excitation spectrum at $\mu=500$ MeV as a function of E_p with different values of Δ/μ in Fig. 1. $\Delta/\mu=0$ (the circles) correspond to the excitation spectrum in the

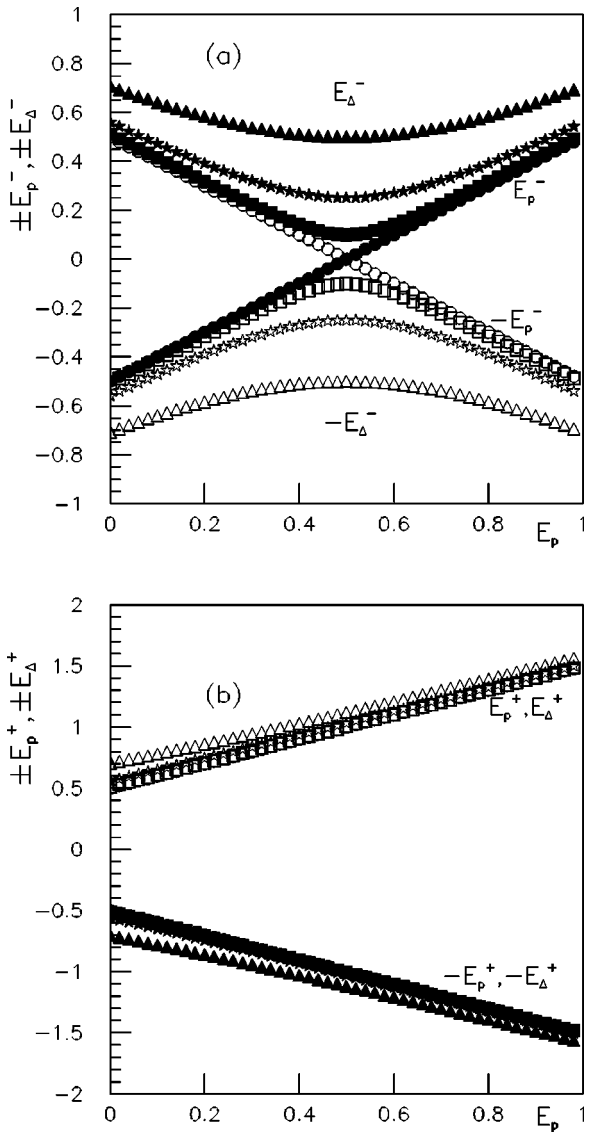

FIG. 1. The excitation spectrum at $\mu=500$ MeV for (quasi)particles and (quasi)holes in (a) and for (quasi)antiparticles and (quasi)antiholes in (b) as a function of E_p with different values of Δ/μ, $\Delta/\mu=0$ (circles), 0.2 (squares), 0.5 (stars), and 1 (triangles). The black and white points are for the particles and holes, respectively.

normal phase, and $\Delta/\mu=0.2$ (the squares), 0.5 (the stars), and 1 (the triangles) correspond to the excitation spectrum in the color superconducting phase. The black points are for the particles and the white points are for the holes. (a) is for the (quasi)particles $E_p^-(E_\Delta^-)$ and (quasi)holes $-E_p^-(-E_\Delta^-)$, and (b) is for the (quasi)antiparticles $-E_p^+(-E_\Delta^+)$ and (quasi)antiholes $E_p^+(E_\Delta^+)$.

It can be easily seen from (a) that the quasiparticles and the quasiholes mix particles and holes, which are called ''Bogoliubons.'' In the normal phase, to excite a pair of particles and holes on the Fermi surface does not need energy, while in the superconducting phase, to excite a pair of quasiparticles and quasiholes at least needs the energy 2Δ when $E_p=\mu$. With increasing Δ, it is found that to excite a quasiparticle needs a larger energy, and the difference between the excitation energies at $E_p\neq\mu$ and that at $E_p=\mu$ becomes smaller.

From (b) we see that to excite an antiparticle is much more difficult, and the diquark condensate has little effect on the excitation spectrum of (quasi)antiparticles and (quasi)antiholes.

B. The calculation of $\ln \mathcal{Z}_{q_3}$

For the third quark which does not participate in the diquark condensate, from Eq. (16), we have

$$\ln \mathcal{Z}_{q_3}=\frac{1}{2}\ln\{\mathrm{Det}(\beta[G_0]^{-1})\}$$

$$=\frac{1}{2}\ln\{\mathrm{Det}(\beta[G_0^+]^{-1})\mathrm{Det}(\beta[G_0^-]^{-1})\}. \quad (30)$$

Using the Dirac matrix, we first perform the determinant in the Dirac space,

$$\mathrm{Det}\,\beta[G_0^+]^{-1}=\mathrm{Det}\,\beta[(p_0+\mu)\gamma_0-\vec{\gamma}\cdot\vec{p}-m]$$

$$=\mathrm{Det}\,\beta\begin{pmatrix}(p_0+\mu)-m & \vec{\sigma}\cdot\vec{p}\\ -\vec{\sigma}\cdot\vec{p} & -(p_0+\mu)-m\end{pmatrix},$$

$$=-\beta^2[(p_0+\mu)^2-E_p^2], \quad (31)$$

and in a similar way we get

$$\mathrm{Det}\,\beta[G_0^-]^{-1}=-\beta^2[(p_0-\mu)^2-E_p^2]. \quad (32)$$

After performing the determinant in the Dirac space, we have

$$\mathrm{Det}\,\beta[G_0^+]^{-1}\mathrm{Det}\,\beta[G_0^-]^{-1}=\beta^2[p_0^2-(E_p+\mu)^2]\beta^2[p_0^2-(E_p-\mu)^2]. \quad (33)$$

Considering the determinant in the flavor, color, spin spaces, and momentum-frequency space, we get the standard expression

$$\ln \mathcal{Z}_{q_3}=N_f\sum_n\sum_{\vec{p}}(\ln\{\beta^2[p_0^2-(E_p+\mu)^2]\}+\ln\{\beta^2[p_0^2-(E_p-\mu)^2]\}), \quad (34)$$

remembering that the color space for the third quark is one dimensional.

C. The calculation of $\ln \mathcal{Z}_{q_{1,2}}$

It is more complicated to evaluate the thermodynamic potential for the quarks participating in the diquark condensate. From Eq. (15), we have

$$\ln \mathcal{Z}_{q_{1,2}}=\frac{1}{2}\ln\mathrm{Det}(\beta G^{-1}). \quad (35)$$

For a 2×2 matrix with elements A, B, C, and D, we have the identity

$$\mathrm{Det}\begin{pmatrix} A & B \\ C & D \end{pmatrix} = \mathrm{Det}(-CB + CAC^{-1}D) = \mathrm{Det}(-BC + DC^{-1}AC). \quad (36)$$

To prove the above equation, we have used

$$\begin{pmatrix} A & B \\ C & D \end{pmatrix} \equiv \begin{pmatrix} 0 & B \\ C & 0 \end{pmatrix}\begin{pmatrix} 1 & C^{-1}D \\ B^{-1}A & 1 \end{pmatrix} \equiv \begin{pmatrix} BC^{-1} & AB^{-1} \\ DC^{-1} & CB^{-1} \end{pmatrix}\begin{pmatrix} 0 & C \\ B & 0 \end{pmatrix}. \quad (37)$$

Replacing A, B, C, and D with the corresponding elements of G^{-1}, we have

$$\begin{aligned} \mathrm{Det}(\beta \mathrm{G}^{-1}) &= \beta^2\,\mathrm{Det}\,D_1 = \beta^2\,\mathrm{Det}\,(-\Delta^+\Delta^- \\ &\quad + \Delta^+[G_0^+]^{-1}[\Delta^+]^{-1}[G_0^-]^{-1}) \\ &= \beta^2\,\mathrm{Det}\,D_2 = \beta^2\,\mathrm{Det}\,(-\Delta^+\Delta^- \\ &\quad + [G_0^-]^{-1}[\Delta^-]^{-1}[G_0^+]^{-1}\Delta^-). \end{aligned} \quad (38)$$

Using the energy projectors $\tilde{\Lambda}_\pm$, we can work out D_1 and D_2 as

$$\begin{aligned} D_1 &= \Delta^2 + \gamma_5[\gamma_0(p_0 - E_p^-)\tilde{\Lambda}_+ + \gamma_0(p_0 + E_p^+)\tilde{\Lambda}_-] \\ &\quad \times \gamma_5[\gamma_0(p_0 - E_p^+)\tilde{\Lambda}_+ + \gamma_0(p_0 + E_p^-)\tilde{\Lambda}_-] \\ &= -[(p_0^2 - E_p^{-2} - \Delta^2)\tilde{\Lambda}_- + (p_0^2 - E_p^{+2} - \Delta^2)\tilde{\Lambda}_+], \\ D_2 &= -\{(p_0^2 - (E_p^-)^2 - \Delta^2)\tilde{\Lambda}_+ \\ &\quad + [p_0^2 - (E_p^+)^2 - \Delta^2]\tilde{\Lambda}_-\}. \end{aligned} \quad (39)$$

Using the properties of the energy projectors, we can get

$$\begin{aligned} D_1 D_2 &= [(p_0^2 - (E_p^-)^2 - \Delta^2)][(p_0^2 - (E_p^+)^2 - \Delta^2)] \\ &= [p_0^2 - E_\Delta^{-2}][p_0^2 - E_\Delta^{+2}]. \end{aligned} \quad (40)$$

With the above equations, Eq. (35) can be expressed as

$$\begin{aligned} \ln \mathcal{Z}_{q_{1,2}} &= \frac{1}{2}\ln[\mathrm{Det}\,\beta G^{-1}] = \frac{1}{4}\mathrm{Tr}\ln[\beta^2 D_1 \beta^2 D_2] \\ &= \frac{1}{4}\{\mathrm{Tr}\ln[\beta^2(p_0^2 - E_\Delta^{-2})] \\ &\quad + \mathrm{Tr}\ln[\beta^2(p_0^2 - E_\Delta^{+2})]\} \\ &= 2N_f \sum_n \sum_p \{\ln[\beta^2(p_0^2 - E_\Delta^{-2})] \\ &\quad + \ln[\beta^2(p_0^2 - E_\Delta^{+2})]\}. \end{aligned} \quad (41)$$

D. The thermodynamic potential

The frequency summation of the free energy

$$\ln \mathcal{Z}_f = \sum_n \ln[\beta^2(p_0^2 - E_p^2)] \quad (42)$$

can always be obtained by performing the frequency summation of the propagator $1/(p_0^2 - E_p^2)$. Differentiate Eq. (42) with respect to E_p:

$$\frac{\partial \ln \mathcal{Z}_f}{\partial E_p} = -2E_p \sum_n \frac{1}{p_0^2 - E_p^2} = \beta[1 - 2\tilde{f}(E_p)], \quad (43)$$

where $\tilde{f}(x) = 1/(e^{\beta x} + 1)$ is the usual Fermi-Dirac distribution function. Then integrating with respect to E_p, one can get the free energy

$$\ln \mathcal{Z}_f = \beta[E_p + 2T\ln(1 + e^{-\beta E_p})]. \quad (44)$$

With the help of the above expression, and replacing

$$\sum_p \rightarrow V\int \frac{d^3p}{(2\pi)^3}, \quad (45)$$

we get the expressions

$$\begin{aligned} \ln \mathcal{Z}_{q_3} &= N_f \beta V \int \frac{d^3p}{(2\pi)^3}[E_p^+ + 2T\ln(1 + e^{-\beta E_p^+}) \\ &\quad + E_p^- + 2T\ln(1 + e^{-\beta E_p^-})], \end{aligned} \quad (46)$$

$$\begin{aligned} \ln \mathcal{Z}_{q_{1,2}} &= 2N_f \beta V \int \frac{d^3p}{(2\pi)^3}[E_\Delta^+ + 2T\ln(1 + e^{-\beta E_\Delta^+}) \\ &\quad + E_\Delta^- + 2T\ln(1 + e^{-\beta E_\Delta^-})]. \end{aligned} \quad (47)$$

Finally, we obtain the familiar expression of the thermodynamic potential

$$\begin{aligned} \Omega &= -T\frac{\ln \mathcal{Z}}{V} \\ &= \frac{\sigma^2}{4G_S} + \frac{\Delta^2}{4G_D} \\ &\quad - 2N_f \int \frac{d^3p}{(2\pi)^3}[E_p + T\ln(1 + e^{-\beta E_p^+}) \\ &\quad + T\ln(1 + e^{-\beta E_p^-}) + E_\Delta^+ + 2T\ln(1 + e^{-\beta E_\Delta^+}) \\ &\quad + E_\Delta^- + 2T\ln(1 + e^{-\beta E_\Delta^-})]. \end{aligned} \quad (48)$$

IV. CONDENSATES AND GAP EQUATIONS

A. Condensates

With the Nambu-Gorkov quark propagator Eqs. (27) and (28), the diquark condensate is generally expressed as

$$\langle \bar{q}^C \gamma_5 q \rangle = \left(iT \sum_n \right) \int \frac{d^3p}{(2\pi)^3} \mathrm{Tr}[\Xi^- \gamma_5]. \quad (49)$$

From general consideration, there should be eight scalar diquark condensates [5,7]. In the case of the NJL-type model, the diquark condensates related to momentum vanish, and there is only one independent 0^+ diquark gap with a Dirac structure $\Gamma = \gamma_5$ for massless quarks, and there exists another 0^+ diquark condensate with Dirac structure $\Gamma = \gamma_0 \gamma_5$ at nonzero quark mass. In our paper we assume the contribution of the diquark condensate with $\Gamma = \gamma_0 \gamma_5$ is small, and we only consider the diquark condensate with $\Gamma = \gamma_5$.

Performing the Matsubara frequency summation and taking the limit $T \to 0$, we get the diquark condensate at finite chemical potential

$$\langle \bar{q}^C \gamma_5 q \rangle = -2\Delta N_c N_f \int \frac{d^3}{(2\pi)^3} \left[\frac{1}{2E_\Delta^-} + \frac{1}{2E_\Delta^+} \right]. \quad (50)$$

For the third quark, its chiral condensate can be evaluated by using the quark propagator in the normal phase,

$$\langle \bar{q}_3 q^3 \rangle = -iT \sum_n \int \frac{d^3p}{(2\pi)^3} \mathrm{Tr}[G_0^+], \quad (51)$$

while for the quarks participating in the diquark condensate, the chiral condensate should be evaluated by using the quark propagator in the color-breaking phase,

$$\langle \bar{q}_1 q^1 \rangle = -iT \sum_n \int \frac{d^3p}{(2\pi)^3} \mathrm{Tr}[G^+]. \quad (52)$$

We have no explicit mass expression for the first two quarks which participate in the diquark condensate. The influence of the diquark condensate has been reflected in the quark propagator. The difference between the first two quarks which participate in the diquark condensate and the third quark which does not participate in the diquark condensate can be read from their chiral condensates and can be defined as

$$\delta = \langle \bar{q}_1 q_1 \rangle^{1/3} - \langle \bar{q}_3 q_3 \rangle^{1/3}, \quad (53)$$

where δ has the dimension of energy. In the case of chiral limit, the quark mass m decreases to zero in the color superconducting phase, and the influence of the diquark condensate on quarks in different colors vanishes.

After performing the Matsubara frequency summation and taking the limit $T \to 0$, we get the expressions of the condensates at $\mu \neq 0$,

$$\langle \bar{q}_3 q^3 \rangle = 4mN_f \int \frac{d^3p}{(2\pi)^3} \frac{1}{2E_p} [\theta(\mu - E_p) - 1],$$
$$\langle \bar{q}_1 q^1 \rangle = 4mN_f \int \frac{d^3p}{(2\pi)^3} \frac{1}{2E_p} [n_p^+ - n_p^-], \quad (54)$$

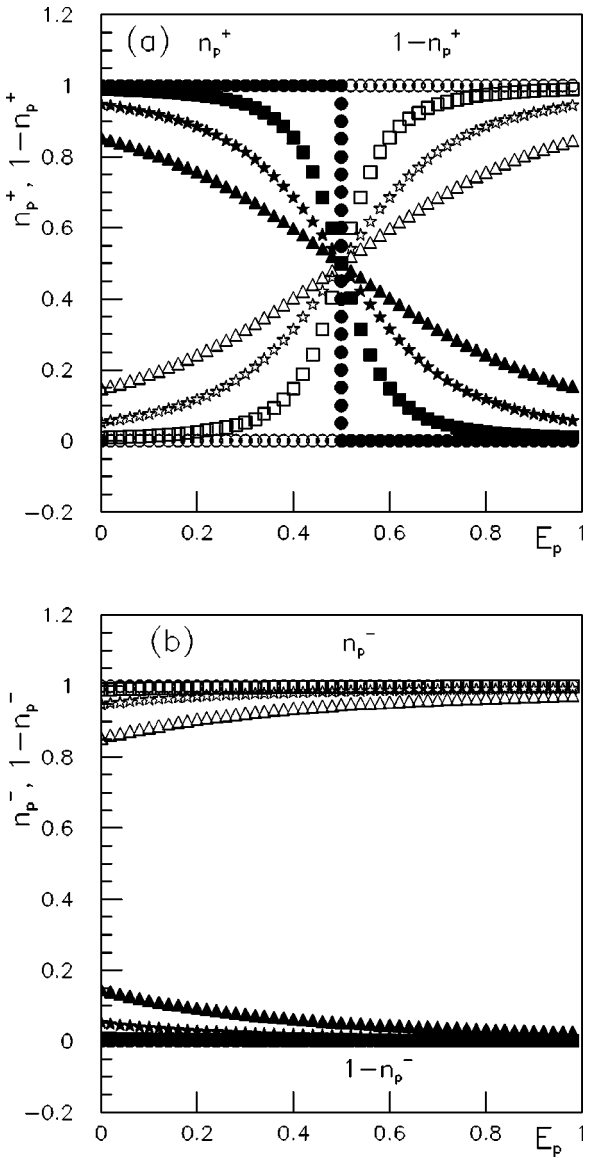

FIG. 2. The occupation numbers for (quasi)particles n_p^+ and (quasi)holes $1-n_p^+$ in (a), and for (quasi)antiparticles n_p^- and (quasi)antiholes $1-n_p^-$ in (b) as a function of E_p with respect to $\Delta/\mu = 0$ (circles), 0.2 (squares), 0.5 (stars), and 1 (triangles). The black and white points correspond to particles and holes, respectively.

where

$$n_p^\pm = \frac{1}{2} \left(1 \mp \frac{E_p^\mp}{E_\Delta^\mp} \right) \quad (55)$$

are the occupation numbers for quasiparticles and quasiantiparticles at $T = 0$. Correspondingly, $1-n_p^\pm$ are the occupation numbers of quasiholes and quasiantiholes, respectively.

We plot the occupation numbers for (quasi)particles n_p^+ and (quasi)holes $1-n_p^+$ in Fig. 2(a), and the occupation numbers for (quasi)antiparticles n_p^- and (quasi)antiholes $1-n_p^-$ in 2(b) as a function of E_p with respect to $\Delta/\mu = 0$

(circles), 0.2 (squares), 0.5 (stars), and 1 (triangles); the black and white points correspond to particles and holes, respectively.

It is seen that the Fermi surface is very sharp in the normal phase $\Delta/\mu=0$, and becomes smooth when diquark condensate appears. The smearing is a consequence of the fact that the ''Bogliubons'' are superpositions of particle and hole states. The smearing of the Fermi surface induces the chiral symmetry restoring at a smaller chemical potential. The larger the diquark condensate is, the smoother the Fermi surface will be. From Fig. 2(b) it can be seen that the occupation numbers for the (quasi)antiparticles (antiholes) in the normal phase or color-breaking phase are not sensitive to the magnitude of the diquark condensate.

B. Gap equations

The two gap equations m and Δ can be derived by minimizing the thermodynamic potential, Eq. (48) with respect to m and Δ,

$$\frac{\partial\Omega}{\partial m}=\frac{\partial\Omega}{\partial\Delta}=0. \tag{56}$$

Taking into account the general expressions for the diquark condensate and chiral condensates, one can get the relations between the chiral gap m and the chiral condensate $\langle\bar{q}q\rangle$, i.e.,

$$\begin{aligned} m&=m_0+\sigma,\\ \sigma&=-2G_S\langle\bar{q}q\rangle. \end{aligned} \tag{57}$$

Here the chiral condensate should perform summation in the color space

$$\langle\bar{q}q\rangle=2\langle\bar{q}_1q^1\rangle+\langle\bar{q}_3q^3\rangle, \tag{58}$$

and the relation between the diquark gap Δ and the diquark condensate $\langle\bar{q}^C\gamma_5 q\rangle$, i.e.,

$$\Delta=-2G_D\langle\bar{q}^C\gamma_5 q\rangle. \tag{59}$$

Substituting Eq. (50) into the above equation, the gap equation for the diquark condensate Eq. (59) in the limit of $T\to 0$ can be written as

$$1=4N_cN_fG_D\int\frac{d^3p}{(2\pi)^3}\left[\frac{1}{2E_\Delta^-}+\frac{1}{2E_\Delta^+}\right]. \tag{60}$$

V. NUMERICAL RESULTS

In this section, through numerical calculations, we will investigate the phase structure along the chemical potential direction, analyze the competition mechanism between the chiral condensate and diquark condensate, and discuss the influence of the color breaking on the quarks in different colors.

Before the numerical calculations, we should fix the model parameters. The current quark mass $m_0=5.5$ MeV, the fermion momentum cutoff $\Lambda_f=0.637$ GeV, and the coupling constant in the color-singlet channel $G_S=5.32$ GeV^{-2} are determined by fitting pion properties. The corresponding constituent quark mass in the vacuum is taken to be $m(\mu=0)=330$ MeV. The coupling constant in the color antitriplet channel G_D can in principle be determined by fitting the nucleon properties. In [26] $G_D/G_S\simeq 2.26/3$ was chosen by fitting the scalar diquark mass of $\simeq 600$ MeV to obtain a realistic baryon mass in the order of $\simeq 900$ MeV. In our case, to investigate the influence of diquark condensate on the chiral phase transition, we will set $G_D/G_S=0,2/3,1,1.2,1.5$, respectively.

A. Phase structure at zero temperature

First, we investigate the phase structure along the chemical potential direction with respect to different magnitudes of G_D/G_S. In the explicit chiral symmetry-breaking case, we define the point at which the chiral condensate has maximum change as the critical chemical potential μ_χ for the chiral phase transition, and the point at which the diquark condensate starts to appear as the critical chemical potential μ_Δ for the color superconductivity phase transition.

The two gaps m (white points) and Δ (black points) determined by Eqs. (57) and (59) are plotted in Fig. 3 as functions of μ with respect to different $G_D/G_S=2/3,1,1.2,1.5$ in 3(a), 3(b), 3(c) and 3(d), respectively. In Fig. 4, they are plotted as functions of the scaled baryon density n_b/n_0, where n_0 is the normal nuclear matter density.

In Fig. 3(a), i.e., in the case of $G_D/G_S=2/3$, we see that in the region where the constituent quark mass keeps its value in the vacuum $m(\mu=0)$, the diquark condensate keeps zero. The chiral phase transition and the color superconductivity phase transition nearly occur at the same chemical potential $\mu_\chi\simeq\mu_\Delta=340$ MeV. The two phase transitions are of first order. In the explicit chiral symmetry-breaking case, there is a small chiral condensate in the color superconductivity phase $\mu>\mu_\chi$. This phenomena has been called the coexistence of chiral and diquark condensate in [10,11]. In this coexistence region, the chiral condensate is small and can be described by the Andersom theorem [15].

In Fig. 3(b), with $G_D/G_S=1$, the diquark condensate starts to appear at $\mu_\Delta=298$ MeV, then chiral symmetry restores at $\mu_\chi=304.8$ MeV. Both μ_Δ and μ_χ are smaller than those in the case of $G_D/G_S=2/3$. In the region from μ_Δ to μ_χ, both chiral and color symmetries are broken, which is called the mixed broken phase. The diquark gap increases continuously from zero to 82 MeV in this mixed broken phase, and jumps up to 152 MeV at the critical point μ_χ. The chiral symmetry phase transition is still of the first order, and the jump of the diquark gap can be regarded as the influence of the first order chiral phase transition.

In Figs. 3(c) and 3(d) we see that by increasing G_D/G_S, the diquark condensate starts to appear at smaller μ_Δ, and chiral symmetry restores at smaller μ_χ, while the width of the region of mixed broken phase, $\mu_\chi-\mu_\Delta$, becomes larger. This phenomena has also been found in Ref. [14] in the random matrix model. It is also seen that by increasing G_D/G_S, the first order phase transition of chiral symmetry restoration becomes the second order one, where the critical

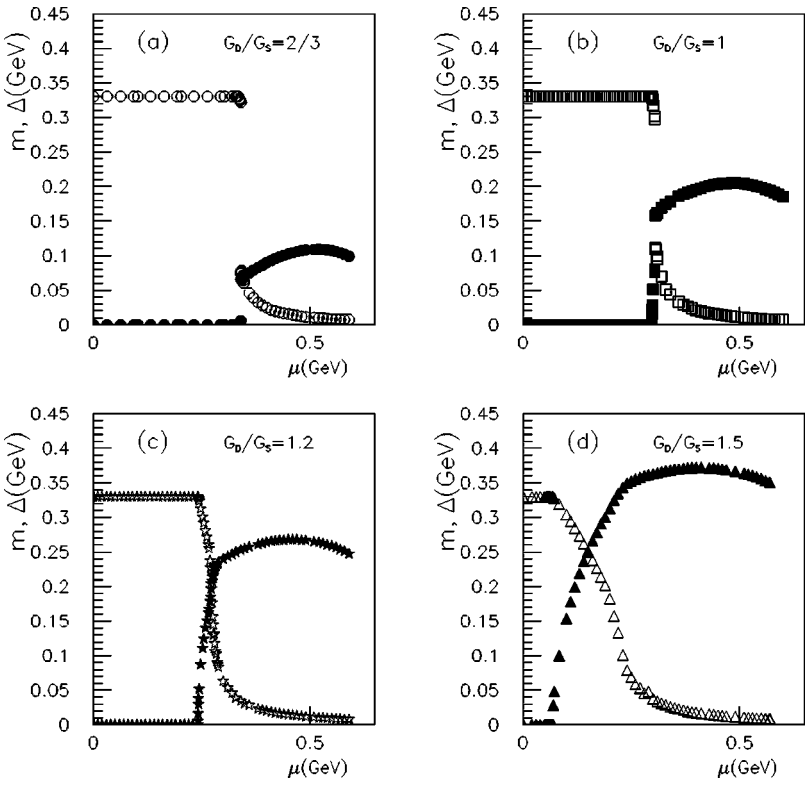

FIG. 3. The two gaps m (white points) and Δ (black points) as functions of chemical potential μ for $G_D/G_S=0,2/3,1,1.2,1.5$, respectively.

point μ_χ is still defined by the maximum change of quark mass m.

We summarize the phase structure along the chemical potential direction: (1) when $\mu<\mu_\Delta$, chiral symmetry is broken; (2) in the region from μ_Δ to μ_χ, both chiral and color symmetries are broken, and (3) when $\mu>\mu_\chi$, chiral symmetry restores partially and the phase is dominated by color superconductivity. The phase transition from the chiral broken phase to the mixed broken phase is of second order, and the phase transition from the mixed broken phase to the color superconductivity phase is of first order for small G_D/G_S, and of second order for large G_D/G_S. The phase structure

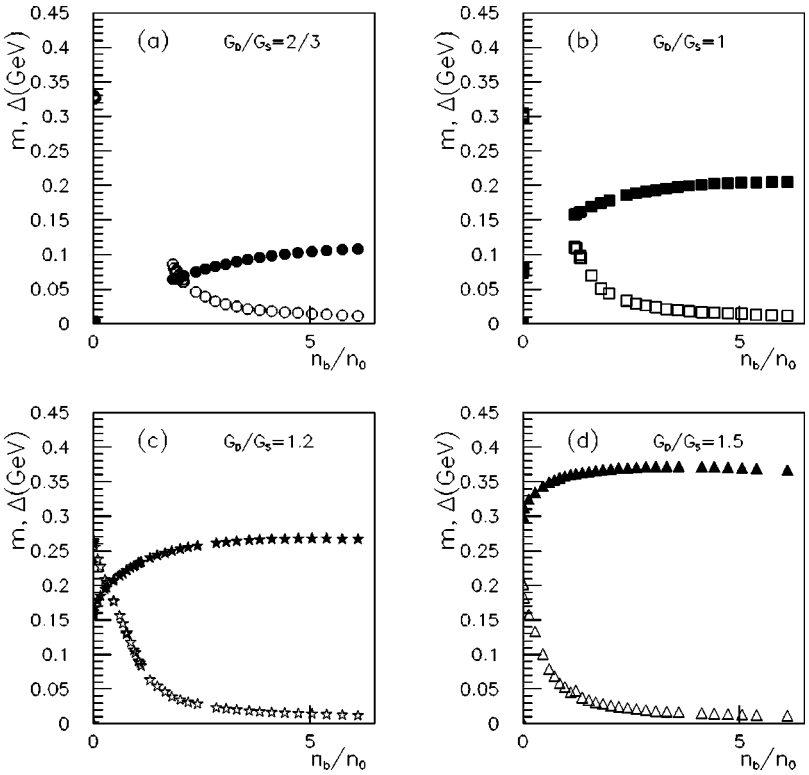

FIG. 4. The two gaps m (white points) and Δ (black points) as functions of the scaled baryon density n_b/n_0 for $G_D/G_S=0,2/3,1,1.2,1.5$, respectively.

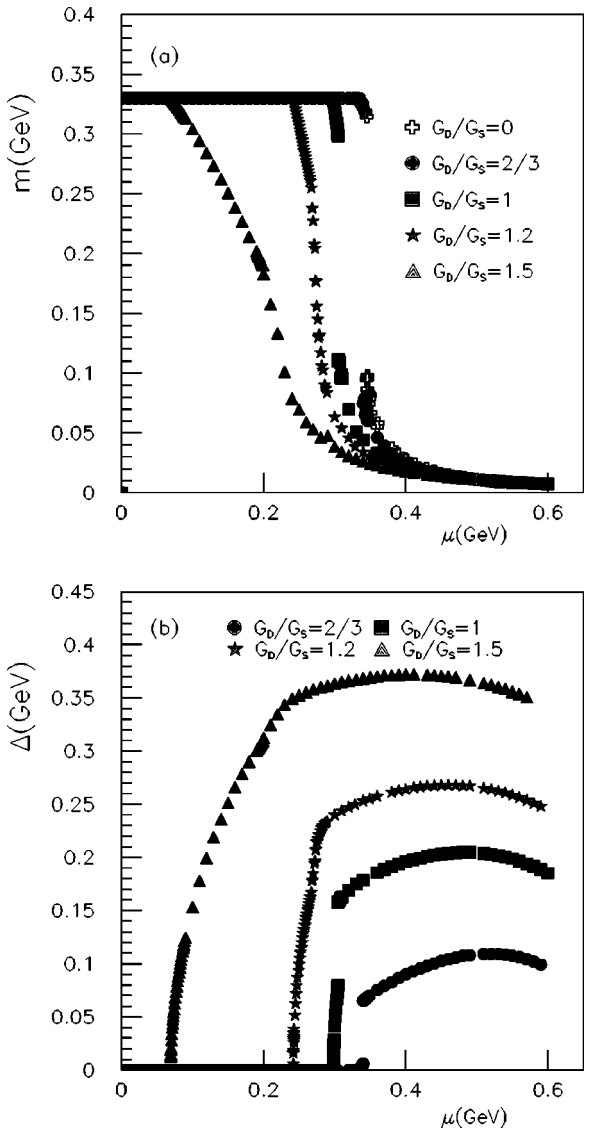

FIG. 5. The gaps m in (a) and Δ in (b) as a function of the chemical potential μ with respect to $G_D/G_S=0,2/3,1,1.2,1.5$, respectively.

depends on the magnitude of G_D/G_S. If G_D/G_S is very small, the diquark condensate will never appear. If $G_D/G_S<1$ but not too small, there will be no mixed broken phase, the chiral phase transition and the color superconductivity phase transition occur at the same critical point $\mu_\chi=\mu_\Delta$, and the two phase transitions are of first order like in [10].

B. The competition between the chiral and diquark condensate

By increasing G_D/G_S, the diquark condensate starts to appear at smaller μ_Δ and chiral symmetry restores at smaller μ_χ, while the width of the mixed broken phase, $\mu_\chi-\mu_\Delta$, increases. In order to understand the competition mechanism and explicitly show how the diquark condensate influences the chiral phase transition, we plot the constituent quark mass m and the diquark gap Δ as functions of μ for different values of G_D/G_S in Fig. 5.

In the case of $G_D/G_S=0$, only chiral phase transition occurs; the thermal system in the mean-field approximation is nearly a free Fermi gas made of constituent quarks. In the limit of $T=0$, there is a very sharp Fermi surface of the constituent quark. When the chemical potential is larger than the constituent quark mass in the vacuum, the chiral symmetry restores, and the system of constituent quarks becomes a system of current quarks. When a diquark gap Δ forms in the case of $G_D/G_S\neq 0$, it will smooth the sharp Fermi surface of the constituent quark. In other words, the diquark pair lowers the sharp Fermi surface and induces a smaller critical chemical potential of chiral restoration.

In Table I we list the chemical potentials μ_Δ, at which the diquark gap starts appearing, and μ_χ, at which the chiral symmetry restores for different values of G_D/G_S. $\mu_F^0=345.3$ MeV is the critical chemical potential in the case of $G_D/G_S=0$. Δ_χ is the value of the diquark gap at μ_χ, and if there is a jump, it is the lower value.

We see that for larger G_D/G_S, the diquark condensate appears at a smaller chemical potential μ_Δ, and the chiral phase transition occurs at a smaller critical chemical potential μ_χ, the gap of the diquark condensate Δ_χ at μ_χ becomes larger, and the region of mixed broken phase becomes wider.

We assume the relation between Δ_χ and μ_χ as

$$\mu_\chi=\mu_F^0-x\Delta_\chi, \tag{61}$$

and the relation between Δ_χ and μ_Δ as

$$\mu_\Delta=\mu_F^0-y\Delta_\chi. \tag{62}$$

In Table I we listed the values of $x=(\mu_F^0-\mu_\chi)/\Delta_\chi$ and $y=(\mu_F^0-\mu_\Delta)/\Delta_\chi$ for different G_D/G_S. It is found that x is almost G_D/G_S independent and equal to 1/2. As for y, it is larger than 1/2 and increases with increasing of G_D/G_S. From Eqs. (61) and (62), we have the relation

TABLE I. The G_D dependence of chemical potentials μ_Δ and μ_χ, $\mu_F^0=345.3$ MeV.

G_D/G_S	μ_Δ (MeV)	μ_χ (MeV)	$\mu_\chi-\mu_\Delta$ (MeV)	Δ_χ (MeV)	$(\mu_F^0-\mu_\chi)/\Delta_\chi$	$(\mu_F^0-\mu_\Delta)/\Delta_\chi$
1	298	304.8	6	82	0.49	0.57
1.2	242	266	24	162	0.49	0.64
1.5	70	190	120	310	0.50	0.89

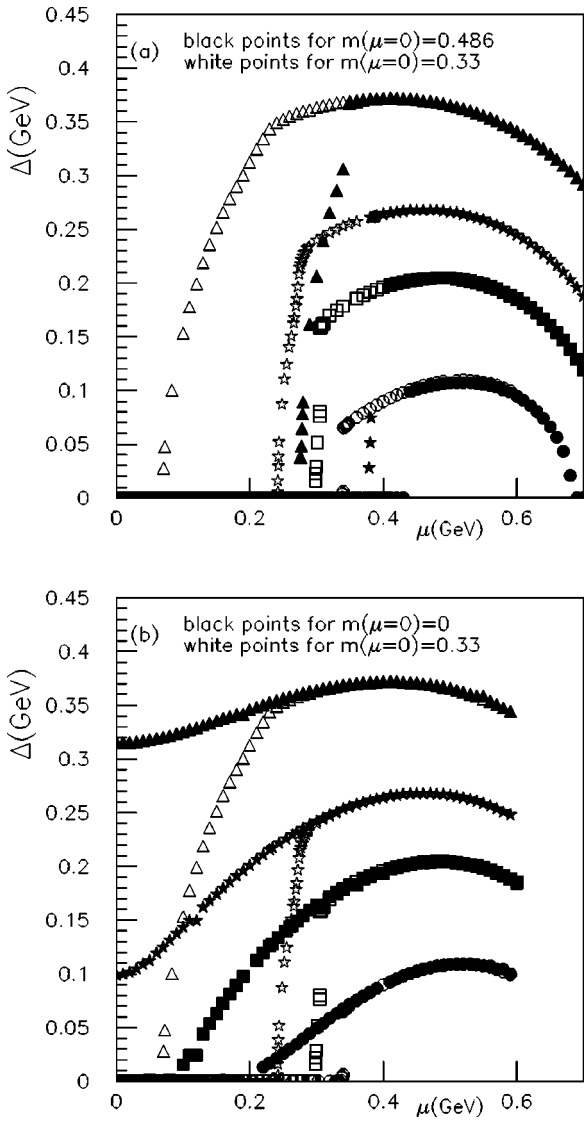

FIG. 6. The influence of the chiral gap on the color superconductivity phase transition in the case of $m(\mu=0)=486$ MeV in (a) and $m(\mu=0)=0$ in (b).

$$\mu_\chi-\mu_\Delta=(y-1/2)\Delta_\chi \tag{63}$$

for the mixed broken phase. With increasing of G_D/G_S, y and Δ_χ increase, and then the width of the mixed broken phase, $\mu_\chi-\mu_\Delta$, becomes larger.

Now we turn to study how the chiral gap influences the color superconductivity phase transition. Firstly, we change the constituent quark mass in the vacuum from 330 MeV to 486 MeV. To fit the pion properties, the coupling constant in the quark-antiquark channel is correspondingly increased from G_S to $1.2G_S$. We plot the diquark gap as a function of μ in Fig. 6(a) for the two vacuum masses and for $G_D/G_S=2/3,1,1.2,1.5$. We find that for the same G_D/G_S, the diquark gap starts to appear at much larger chemical potential μ_Δ when the vacuum mass increases from 330 MeV to 486 MeV.

Then we withdraw the quark mass, i.e., taking $m=0$ even in the vacuum. We plot the diquark gap as a function of μ in Fig. 6(b) for $m(\mu=0)=0$ and 330 MeV and for $G_D/G_S=2/3,1,1.2,1.5$. We find that for any G_D/G_S, the diquark condensate starts to appear at a much smaller chemical potential μ_Δ for $m(\mu=0)=0$ compared with $m(\mu=0)=330$ MeV.

From Figs. 6(a) and 6(b) we can see that the quark's vacuum mass only changes the critical point of color superconductivity μ_Δ. The diquark gaps for different quark's vacuum mass coincide in the overlap region of the color superconductivity phase, where chiral symmetry is partially restored.

From the influcence of the diquark gap on the chiral phase transition and the influence of the chiral gap on the color superconductivity phase transition, it is found that there does exist a strong competition between the two phases. The competition starts at μ_Δ and ends at μ_χ. We call the mixed broken phase the competition region, which becomes wider by increasing G_D/G_S. This competition region is the result of the diquark gap smoothing the sharp Fermi surface of the constituent quark. If the attractive interaction in the diquark channel is too small, there will be no diquark pairs, the system will be in the chiral-breaking phase before μ_χ, and in the chiral symmetry restoration phase after μ_χ. If the attractive interaction in the diquark channel is strong enough, diquark pairs can be formed and smooth the sharp Fermi surface, and a smaller critical chemical potential of chiral symmetry restoration is induced.

C. The influence of color breaking on quarks' properties

Finally, we study how the diquark condensate influences the quark properties. In the normal phase, the quarks in different colors are degenerate. However, in the color-breaking phase, the first two quarks are involved in the diquark condensate, while the third one is not.

The quark mass m that appeared in the formulas of this paper is the mass for the third quark which does not participate in the diquark condensate. We have seen from Fig. 5(a) that the diquark condensate greatly influences the quark mass m in the competition region $\mu_\Delta<\mu<\mu_\chi$. In the color-breaking phase, i.e., when $\mu>\mu_\Delta$, the quark mass m in different cases of G_D decreases slowly with increasing μ, and reaches the same value at about $\mu=500$ MeV.

The difference of the chiral condensates for quarks in different colors δ defined in Eq. (53) is shown in Fig. 7 as a function of the chemical potential μ with respect to $G_D/G_S=2/3,1,1.2,1.5$. It is found that in any case where δ is zero before μ_Δ, then δ begins to increase at μ_Δ and reaches its maximum at μ_χ, and then starts to decrease after $\mu>\mu_\chi$ and approaches zero at about $\mu=500$ MeV. When $\mu>500$ MeV, δ becomes negative. With increasing G_D, $\delta(\mu_\chi)$ increases from 1 MeV for $G_D/G_S=2/3$ to 13 MeV for $G_D/G_S=1.5$. Comparing with the magnitude of the diquark condensate, δ is relatively small in the color superconductivity phase.

VI. CONCLUSIONS

In summary, in an extended NJL model and considering only the attractive interactions in the 0^+ color-singlet quark-

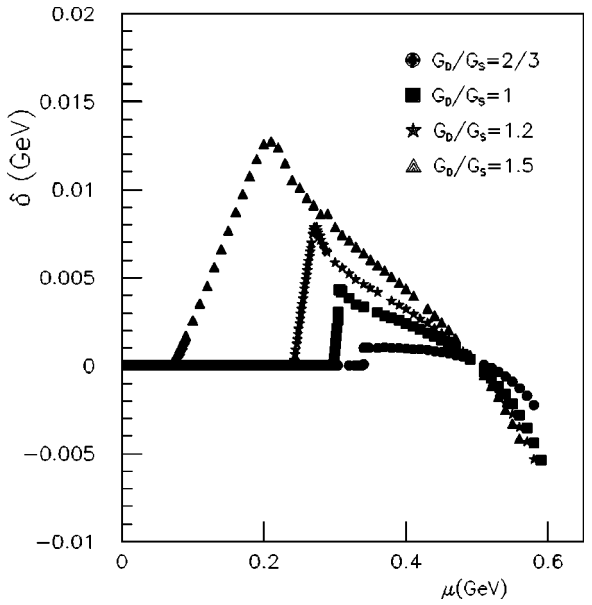

FIG. 7. The difference of the chiral condensates for quarks in different colors δ as a function of the chemical potential μ with respect to $G_D/G_S=0,2/3,1,1.2,1.5$, respectively.

antiquark channel and color-antitriplet diquark channel, the Nambu-Gorkov form of the quark propogator has been evaluated with a dynamical quark mass. The Nambu-Gorkov massive propagator makes it possible to extend the Green-function approach to the moderate baryon density region, and the familiar expression of the thermodynamic potential has been reevaluated by using the massive quark propagator. In this paper we have neglected another scalar diquark condensate with Dirac structure $\gamma_0\gamma_5$, which is assumed to be small.

The phase structure along the chemical potential direction has been investigated. The system is in the chiral-breaking phase before μ_Δ, in the color superconducting phase after μ_χ, and the two phases compete with each other in the mixed broken phase with width $\mu_\chi-\mu_\Delta$. The width depends on the magnitude of G_D/G_S. If G_D/G_S is small, the width is zero, and the chiral phase transition and the color superconductivity phase transition that occur at the same chemical potential. The width increases with increasing of G_D/G_S. The competition mechanism has been analyzed by investigating the influence of the diquark condensate on the sharp Fermi surface. The diquark condensate smoothes the sharp Fermi surface, and induces the chiral phase transition that occurs at a smaller chemical potential, and the diquark can be formed more easily. The phase transition is of second order from the chiral symmetry broken phase to the mixed broken phase, and the phase transition from the mixed broken phase to the partial chiral symmetry phase, i.e., the color superconductivity phase is of first order for small G_D/G_S, and is of second order for large G_D/G_S.

The influence of the diquark condensate on the properties of quarks in different colors has also been investigated. It is found that the difference of the chiral condensates between quarks in different colors induced by the diquark condensate is very small.

ACKNOWLEDGMENTS

One of the authors (M.H.) thanks Dr. Qishu Yan for valuable discussions. This work was supported in part by China Postdoctoral Science Foundation, the NSFC under Grant Nos. 10105005, 10135030, and 19925519, and the Major State Basic Research Development Program under Contract No. G2000077407.

[1] M. Alford, K. Rajagopal, and F. Wilczek, Phys. Lett. B **422**, 247 (1998).
[2] R. Rapp, T. Schäfer, E.V. Shuryak, and M. Velkovsky, Phys. Rev. Lett. **81**, 53 (1998).
[3] D. Bailin and A. Love, Phys. Rep. **107**, 325 (1984).
[4] K. Rajagopal and F. Wilczek, hep-ph/0011333.
[5] R.D. Pisarsiki and D.H. Rischke, Phys. Rev. D **60**, 094013 (1999).
[6] R.D. Pisarski and D.H. Rischke, Phys. Rev. D **61**, 074017 (2000).
[7] R.D. Pisarski and D.H. Rischke, Phys. Rev. Lett. **83**, 37 (1999).
[8] T. Schäfer, Phys. Rev. D **65**, 074006 (2002).
[9] M. Rho, E. Shuryak, A. Wirzba, and I. Zahed, Nucl. Phys. **A676**, 273 (2000).
[10] J. Berges and K. Rajagopal, Nucl. Phys. **B538**, 215 (1999).
[11] J. Berges, Nucl. Phys. **A642**, 51 (1998).
[12] T.M. Schwarz, S.P. Klevansky, and G. Papp, Phys. Rev. C **60**, 055205 (1999).
[13] G.W. Carter and D. Diakonov, Phys. Rev. D **60**, 016004 (1999).
[14] B. Vanderheyden and A.D. Jackson, Phys. Rev. D **62**, 094010 (2000).
[15] B.O. Kerbikov, hep-ph/0106324.
[16] R. Rapp, T. Schafer, E.V. Shuryak, and M. Velkovsky, Ann. Phys. (N.Y.) **280**, 35 (2000).
[17] K. Langfeld and M. Rho, Nucl. Phys. **A660**, 475 (1999).
[18] F. Gastineau, R. Nebauer, and J. Aichelin, Phys. Rev. C **65**, 045204 (2002).
[19] M. Buballa, J. Hošek, and M. Oertel, Phys. Rev. D **65**, 014018 (2002).
[20] M. Buballa, and M. Oertel, hep-ph/0109095.
[21] D. Ebert, K.G. Klimenko, and H. Toki, Phys. Rev. D **64**, 014038 (2001).
[22] D. Ebert, K.G. Klimenko, H. Toki, and V. ch. Zhukovsky, Prog. Theor. Phys. **106**, 835 (2001).
[23] D. Ebert, V.V. Khudyakov, V.ch. Zhukovsky, and K.G. Klimenko, Phys. Rev. D **65**, 054024 (2002).
[24] Y. Nambu and G. Jona-Lasinio, Phys. Rev. **122**, 345 (1961); **124**, 246 (1961).
[25] H. Reinhardt, Phys. Lett. B **244**, 316 (1990).
[26] D. Ebert, L. Kaschluhn, and G. Kastelewicz, Phys. Lett. B **264**, 420 (1991).

[27] D. Ebert, Yu.L. Kalinovsky, L. Münchow, and M.K. Volkov, Int. J. Mod. Phys. A **8**, 1295 (1993).
[28] U. Vogl, Z. Phys. A **337**, 191 (1990).
[29] R.T. Cahill, J. Praschifka, and C.J. Burden, Aust. J. Phys. **42**, 161 (1989).
[30] J. Kapusta, *Finite-Temperature Field Theory* (Cambridge University Press, Cambridge, England, 1989).
[31] M.L. Bellac, *Thermal Field Theory* (Cambridge University Press, Cambridge, England, 1996).